

## Part I: Experimental studies on a pulverised fuel stove

C.S. Bhaskar Dixit<sup>a,\*</sup>, P.J. Paul<sup>b</sup>, H.S. Mukunda<sup>b</sup>

<sup>a</sup>Department of Mechanical Engineering, Bapuji Institute of Engineering and Technology, Davanagere 577 004, India

<sup>b</sup>Combustion Gasification and Propulsion Laboratory, Indian Institute of Science, Bangalore 560 012, India

Received 23 November 2004; received in revised form 9 December 2005; accepted 20 January 2006

Available online 29 March 2006

### Abstract

This paper is concerned with development of a pulverised fuel stove with improved conversion efficiency and minimal emissions at near constant power level without the use of external power. The design originates from a cylindrical sawdust stove with a central porthole being lit from the bottom. Such a stove will have a flame in port with enhanced sooting tendency. For similar configuration, stable premixed combustion behaviour of the combustible gases from the port of the fuel block (known as the gasification mode) has been achieved by use of air supply through a thin slot at the bottom, for at least 30 min of stove operation. In order to ensure stable combustion of the gases at exit, a metal device is used. In an attempt to extend gasification duration, studies are conducted in single port configuration having air entry from the bottom with a horizontal baffle to control the flow rate. This configuration worked in gasification mode for about 20 min but there have been problems of flame extinction. To overcome these drawbacks multi-port design with vertical air entry is employed with success.

The stove has exhibited conversion efficiency in excess of 37% due to well focused nature of flame at exit. CO emission factors are about 12 g (kg fuel)<sup>-1</sup>, a performance superior to conventional biomass stoves (~45 g kg<sup>-1</sup>). NO<sub>x</sub> emission factors are about 1 g kg<sup>-1</sup> fuel which falls in the range of reported data for NO<sub>x</sub>. Studies with different pulverised leafy fuels have indicated these fuels have lower volatile release rates and therefore exhibit lower power level operation for a given port configuration compared to sawdust fuel.

© 2006 Elsevier Ltd. All rights reserved.

**Keywords:** Cook stoves; Biomass combustion; Pulverised fuels; Crop residues; Pollutant emissions

### 1. Background

Biomass is used as a cooking fuel in (a) remote small communities due to sheer necessity since the state cannot provide other fuels of choice at locally affordable prices as in cities, (b) villages in developing nations have no access to fuels such as LPG, but have to depend on field collected biomass residues and (c) urban poor located in slums who need to depend on collection of garden wastes, dry kitchen wastes and avenue tree droppings in addition to purchasing low grade fire wood. Half the world population depends on these sources.

Fire wood is considered a fuel of choice amongst the variety of biomass available; other agricultural residues are used only if fire wood is unavailable. The problems of using other agro-residues are that the material is small in size and

burns up fast. This will imply very fluctuating power levels, fast burn up and therefore much greater periodicity in feeding and more attention. This technical problem of using fine agricultural residues and tree droppings including leafy biomass as candidates for domestic fuel has not been addressed at all; it is not that devices that use fine biomass material for domestic applications do not exist. But they are used only for sawdust. They were not contemplated for use with any other biomass. The various bio-fuels such as wood and crop residues are not significantly different in their structure and energy content. The loose biomass burns up faster emitting more products of incomplete combustion compared to solid biomass. Pulverisation would convert these multiple fuels into common physical form (with possibility of controlled combustion) and they can be used in sawdust like stoves.

In the case of sawdust generated in timber processing units, a stove design has been prevalent over several decades in many countries. This stove is called the tube

\*Corresponding author.

E-mail address: [dixit@cgpl.iisc.ernet.in](mailto:dixit@cgpl.iisc.ernet.in) (C.S.B. Dixit).

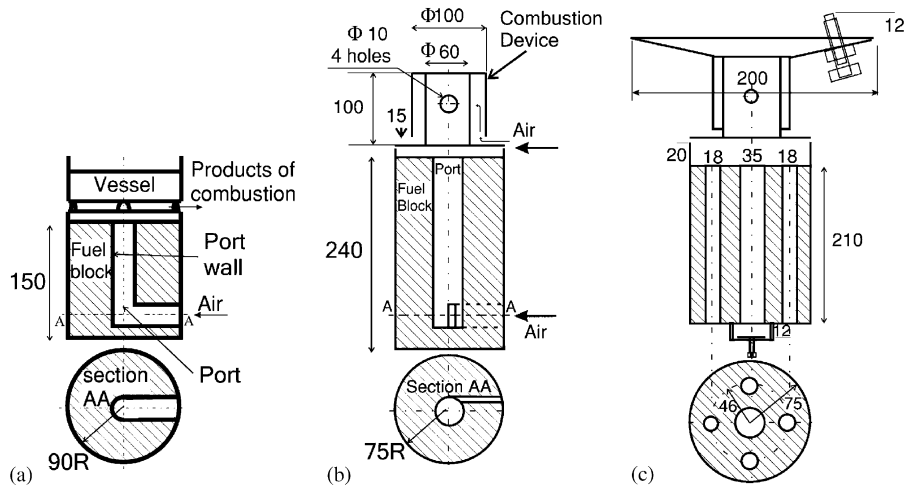


Fig. 1. Schematic of stoves for pulverised fuel.

stove. Its scientific exploration was made only recently by Mukunda et al. [1]. Fig. 1(a) shows a classical tube stove.

The fuel port, wetted with small amount of liquid fuel like kerosene, is ignited at the top, first and bottom air inlet region next. Hot product gases thus generated traverse the port supplying heat to port wall causing pyrolysis of the biomass resulting in volatile release. The volatiles released enter the port where they receive air from air inlet and burn in the port in diffusion mode. The resulting flame at the port exit is fuel rich in nature. This is due to incomplete mixing in the port. Also, arrangement for fuel vapour to receive additional air at exit is not provided. This mode of stove operation is referred to as *combustion mode*. The heat transferred from the flame to the surface of the fuel block causes pyrolysis of the fuel block. With time, the pyrolysis front moves into the fuel block.

If horizontal segment was larger, lower portion of the stove generated large amounts of heat resulting in large amount of volatilisation. Almost from the beginning, the power level became so large that the stove functioned in a highly fuel rich state and unburnt products escaped into surroundings. This obviously caused sooting of the stove.

Mukunda et al. [1] have conducted experiments over a range of parameters like the height-to-port diameter ratio, outer-to-port diameter ratio and determined the power level dependence on the port diameter as well as the above-mentioned ratios, and also determined from the rate of propagation of the pyrolysis front, the web required to meet the demand of a specific burn time. From these data, correlations have been generated for designing a stove for a given power level and a burn time. They have brought up the use of multiple ports but not adequately addressed the performance behaviour. This stove has formed the starting point for experimental studies made in the present work. Mukunda et al. [1] have examined the classical tube stove shown in Fig. 1(a) to ensure (a) smooth ignition, (b) good combustion with little soot or smoke, (c) as high an efficiency as possible, (d) a power level of 2–3 kW, and (e)

the possibility of using different vessels and shapes. The relative diameter of the port and the horizontal segment that draws in the air was not studied in this work. The bottom horizontal segment had the same dimension as the vertical portion. In this configuration it was found that having exposed horizontal segment of fuel, shorter than the fuel web thickness for volatilisation helped causing smooth ignition.

## 2. Experimental tools

Fig. 1(b) shows a representative single port stove configuration used during present experimentation. The typical configuration of pulverised fuel stove consisted of a vertical central port with horizontal air inlet(s) at bottom. The stove was prepared by packing sawdust or pulverised fuel into a cylindrical metallic container. The fuel block thus prepared had a central port and horizontal air inlet(s) at the bottom for providing air entry. With reduced size air inlet, the amount of air inducted into the port is reduced. Under the conditions of reduced availability of air in the port, the volatiles released through the walls of the port do not burn immediately with air, but only mix with it since the mixture will be very rich. The mixture then moves up till the outlet is reached. It will burn in a partially premixed mode over the fuel block and the flaming process is strictly limited to the top region. During this phase the central port is physically red hot on its inner surface, but with no gaseous flame in the port, generates a combustible gaseous fuel-air mixture and burns at the outlet. This phase of operation is called the *gasification mode*. Like in the case of combustion mode, the condensed phase processes include the formation of a pyrolysis front and its movement inside the fuel block. In addition, it must be noted that the gases that issue from the pyrolysis front are passing through the hot char bed and hence the process of reaction of the gases from pyrolysis with the red hot char lead to products that are similar to a normal gasification process [2]—CO, H<sub>2</sub>

and  $\text{CH}_4$  apart from more complex compounds of C–H–O. This is similar to smoldering combustion phenomena discussed in literature [3–6]. The premixed gas out of the port of the fuel block needs additional air for combustion. This process, when stabilised with the addition of a combustion device of the kind shown in the Fig. 1(b), leads to a flame of exemplary quality at the port exit for part of combustion duration.

Experiments are conducted using sun-dry sawdust (10% moisture) sourced from local sawmill. Pulverised fuel is prepared from various leafy biomass separately collected from tree fallings. The leafy biomass was pulverised using hammer mill of capacity  $30 \text{ kg h}^{-1}$ . A mesh size of 3 mm was used giving an average particle size of 1 mm. Pulverised fuel thus generated can be loaded into stove to obtain performance similar to sawdust stove.

A strain gauge-based weighing machine (15 kg range and 0.5 g least count) with digital display and RS-232 output which could communicate mass data to personal computer is used for measurement of instantaneous mass of fuel during stove operation. ASCII Data is transmitted to the computer through RS-232 interface.

Temperature measurements were made in c-phase as well as g-phase of the stove. The c-phase temperature measurement was made using K type mineral wool insulated thin thermocouples (100  $\mu\text{m}$  diameter), R type 50  $\mu\text{m}$  bare wires with different mounting techniques were used for c-phase and g-phase measurements and R-type 100  $\mu\text{m}$  bare wires with suitable mounting techniques for g-phase measurements. K type shielded thermocouple was used for g-phase measurements during exploratory phase of experimentation. All readings were corrected for radiation.

G-phase composition was analysed for  $\text{CO}$ ,  $\text{CO}_2$ ,  $\text{CH}_4$ ,  $\text{O}_2$  and  $\text{H}_2$ . Instrument is calibrated using standard gas of known composition (by gas chromatography).

Experiments were conducted to determine emission factors of pollutants, carbon monoxide and oxides of nitrogen. Calculations procedure for emission factors is covered in [7]. Emission measurements were made using standard hood design described in CIS 1315 z (Part 1) 1991, Annex-2 of Bureau of Indian Standards [8]. Gas analyser used for emission measurements was capable of analysing  $\text{CO}$ ,  $\text{CO}_2$  and  $\text{O}_2$ . The details of measurement scheme can be found in [9].

### 3. Single port studies

Single port studies on a pulverised fuel stove of power level between 2 and 3 kW (amounting to  $0.45\text{--}0.7 \text{ kg h}^{-1}$  of sawdust with slightly higher rates for fuels with higher ash content) with the burn duration of about an hour is described in this section. The criteria for selection of port diameter and aspect ratio (AR) for the required power level and burn duration are set out in [10]. Based on these criteria, it was deduced that pulverised fuel stove with a port diameter of about 40 mm and AR in the range of 4–6 would meet the power demand noted above. A fuel web

thickness of 55–65 mm would account for the burn duration.

The fuel block would begin functioning with flame in port. Once ignition procedure got completed and the horizontal limbs became red hot indicating the initiation of pyrolysis over the entire span of horizontal limbs (in a maximum of 7–8 min), it was observed that the flame in the port disappeared. Volatiles released during pyrolysis of fuel block burnt at the exit. This phenomenon akin to gasification continued for over 30 min, during which the flame quality (characterised by absence of smoke, soot and yellow tongues of flame) at the port exit was *excellent*. Preliminary observations like placing water filled vessel over the stove confirmed the non-sooty nature of the flame. The stove functioned at a constant power level of about 1.6 kW. The part-premixed part-diffusion flame at the exit of port became progressively intense and shorter in height and beyond 30 min or so, flames at the exit flashed back into the port. This phenomenon was some times accompanied by a barely audible sound and a mild shower of sparks. The smooth contours of gasification flame broke up into ragged mildly sooty tongues leading to combustion mode operation. This functioning was sufficiently intriguing to prompt further investigation into the process with an aim to understand the reasons for flash back and try to prolong the gasification duration to the extent possible.

The flash back event originated from fuel port exit. Therefore, to establish the conditions of fuel port that would cause flame flash back, It was thought necessary to continuously monitor the composition of g-phase in the region below the port exit so that g-phase compositional variations could be captured. Visual observation of the fuel port during the gasification mode operation of the stove had indicated a gradual upward progress of red hot char zone along the port surface. This increase in surface temperature might contribute to creation of conditions conducive to flash back. It was surmised that port surface temperature data at locations immediately below fuel port exit would hopefully reveal the reasons for the occurrence.

Therefore, the fuel port surface temperatures along with composition of gases in the region below fuel port exit were continuously monitored in a stove geometry known to operate in gasification mode for part of the burn time from earlier experience. The dimensions are shown in the schematic diagram inset to Fig. 2. Weight loss data of the stove was also acquired to obtain the power level of operation. The fuel port had 32 mm diameter and Three tangential inlets of size  $15 \text{ mm} \times 6 \text{ mm}$  were used. During the experiment, temperatures of fuel port surface and of points 5 mm radially outwards from surface into the condensed phase were measured at two locations on port surface vertically separated by 25 mm with the upper measurement level 40 mm below fuel port exit. For temperature measurement in the condensed phase, 120  $\mu\text{m}$  bead size R type thermocouples mounted on biomass sticks were used.

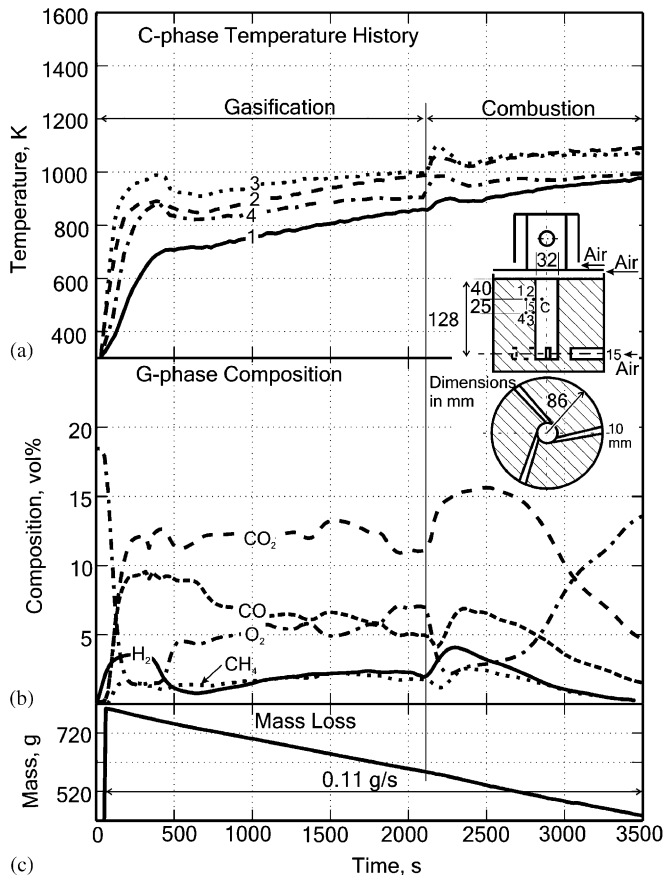


Fig. 2. C-phase temperature and g-phase composition measurement (port diameter = 32 mm AR 4): (a) shows condensed phase temperature history measured using R type 50  $\mu\text{m}$  diameter thermo-couples at locations 1–4 (1–5 mm from port wall, 40 mm below exit, 2—On port wall, 40 mm below exit, 3 on port wall, 65 mm below exit, 4–5 mm from port wall, 65 mm below exit) shown in sectional elevation of the stove. (b) shows simultaneously acquired g-phase composition at location (5 mm from port wall into gas phase, 40 mm below exit). (c) indicates mass loss as a function of time during experiment.

G-phase composition was also measured at a location C which is 5 mm into g-phase, as shown in the sketch, 40 mm below tube exit. The weight loss data, shown in Fig. 2(c) indicates that power level of operation of the stove is nearly constant for the entire duration.

Consider the fuel port surface temperature data presented in Fig. 2(a).  $T_2$ , surface temperature a diameter below fuel port exit, attained 830 K after initial transients as the stove settled down to gasification mode operation. During this mode,  $T_2$  increased gradually until it reached 990 K recording an increase of 160 K in 35 min of operation. At that instant, flame hitherto stabilised at port exit, flashed back into the fuel port. The event was captured by a sharp increase in  $T_2$  by 40 K. It appears 990 K is a threshold port surface temperature in the region below port exit which, once crossed, would permit flame flash back.

$T_2$  increased at a faster rate than  $T_3$  during gasification mode operation.  $T_3$ , 25 mm upstream of  $T_2$ , was higher than  $T_2$  by 35 K initially. This difference kept decreasing

with  $T_3$  becoming equal to  $T_2$  at flash back. During combustion mode these two temperatures remained equal. It appears during combustion mode operation c-phase surface temperatures may be more uniform spatially in the vertical direction than gasification mode.

C-phase radial temperature differences  $T_2 - T_1$  and  $T_3 - T_4$  remained constant at 130 and 100 K, respectively, indicating constant heat flux into c-phase at a given vertical level in the stove.

From the composition record shown in Fig. 2(b) it is seen that, the beginning of gasification mode of operation, confirmed visually by the absence of flame in the port, was indicated by a small but quick increase in oxygen to 4.5% as seen in Fig. 2(b) indicating the formation of a fuel rich air fuel mixture at the measured location. During this mode, oxygen gradually increased to about 7% at which flash back occurred leading to a quick drop in oxygen to 2% due to its consumption within the port and associated increase of carbon dioxide. Oxygen increase beyond 2500 s is inferred to be due to reduced air restriction caused by the removal of the ash layer and char oxidation around the inlets that permitted more air into the port.

The equivalence ratio of the mixture is calculated from the measured composition and plotted in Fig. 3 assuming no higher hydrocarbons or other fuel components were present.

It shows that during gasification mode operation, equivalence ratio of mixture at the measured location fluctuated from 1.4 to 1.8. After 30 min of operation it dropped from 1.4 to 1 in 2 min. For the next 3 min it stayed at unity and at the end of 35th min flash back occurred leading to combustion mode operation confirmed visually by noting the presence of flame in the port.

Thus, the movement of equivalence ratio towards unity in the region immediately below the fuel port exit may be one of the causes for flash back. This implies that a fuel release pattern where volatiles are released at larger rates

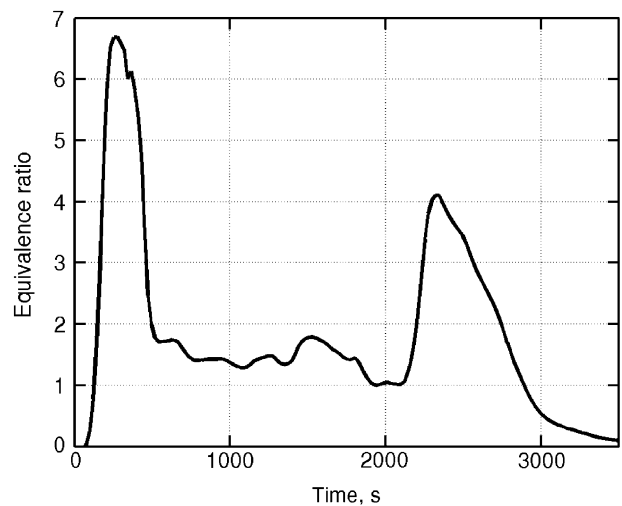


Fig. 3. G-phase equivalence ratio at a station 40 mm below fuel port exit as a function of burn time.

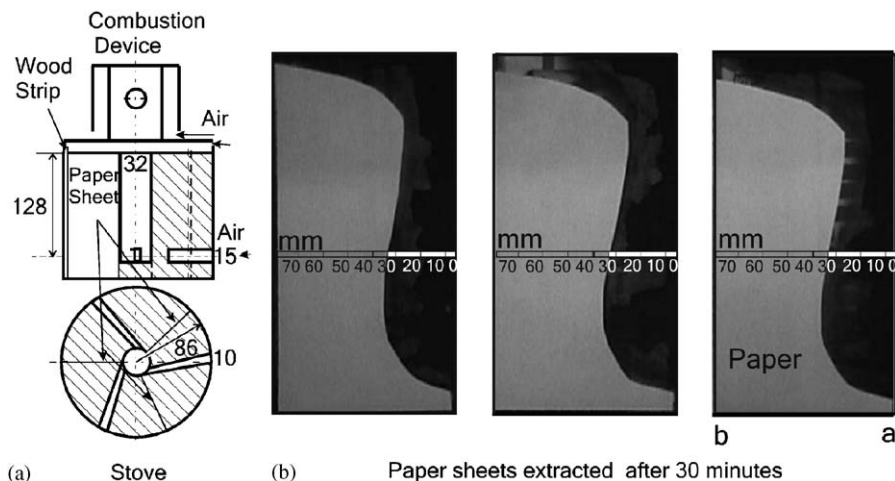


Fig. 4. Symmetry in propagation of pyrolysis front (port diameter = 32 mm, AR 4). The paper sheets were extracted 30 min after initiation of combustion: (a) refers to port wall and (b) refers to outer wall.

from bottom region may be a feature for gasification mode of operation in the stove.

To confirm whether fuel release was indeed larger in stoves operating in gasification mode, it was necessary to examine the vertical fuel release pattern in the stove during gasification mode. Towards this, pyrolysis front positions were determined at three azimuthal positions by inserting paper sheets as shown in Fig. 4(a).

The stove operated in a gasification mode for the first 30 min after which stove was put off to facilitate removal of paper sheets. Paper sheets extracted from the stove are presented in Fig. 4(b). The char zone on the paper sheet is indicative of the region over which pyrolysis was complete. The border between char zone and unburnt paper represents the pyrolysis front. This is found to be about 2–3 mm in width. The following observations can be made from Fig. 4(b):

- The pyrolysis front moved by same amounts at the corresponding vertical locations in all the three char profiles implying circumferentially uniform volatile release.
- In the bottom region, pyrolysis front had advanced into c-phase by a greater extent compared to upper levels. This indicates that during gasification mode operation, volatile release rates in the bottom region are higher than that in the regions above.
- Profiles shown in Fig. 4(b) indicate that the pyrolysis front had moved through a distance of 30 mm at the end of 30 min at mid height of the stove. This indicates an average pyrolysis front movement rate of  $60 \text{ mm h}^{-1}$  during first 30 min of stove operation at mid height during the gasification mode operation.
- There was some amount of downward regression of pyrolysis front around the port indicating increased influx of fuel vapours into the port in the region immediately below fuel port exit during gasification mode operation. This influx, which was present during

earlier part of stove operation, may also help to maintain lower air-to-fuel ratio in the region immediately below fuel port exit.

The average propagation rate was determined as distance moved by pyrolysis front in a known time. The position of pyrolysis front is available as interface between char zone and unburnt paper. pyrolysis zone, indicated by the yellowed region in the paper sheet shown in Figs. 5(a) and (b) was found to be 2–3 mm thick. Results are presented in Fig. 6.

The average propagation rates obtained vary between 25 and  $80 \text{ mm h}^{-1}$ . Time averaged propagation rates obtained for larger time duration (60 min) are lower compared to shorter duration (30 min) at corresponding heights. Propagation rate in the bottom region is seen to be higher compared to upper region. Swirl effects in the bottom region might make a difference by causing particle erosion in the bottom region.

In one of the experiments made for location of pyrolysis front the stove of AR = 4, paper sheet was inserted into the stove along with nine thermocouples attached to it at known radial locations at mid height of the stove.

The thermocouple #5 in Fig. 7 that was nearest to pyrolysis front indicated a temperature of 588 K at the instant the paper sheet was pulled out. It is therefore inferred that the pyrolysis temperature is about  $588 \pm 20 \text{ K}$ , the 20 K indicated here being the temperature variation over 2 mm, the pyrolysis zone thickness as seen from the charred paper sheets. Therefore, the attainment of a temperature of 588 K within the c-phase is assumed to signify location of the middle region of pyrolysis activity. From the known temperature distribution at all times and known thermocouple locations, propagation rates are calculated.

The temporal temperature distribution is presented in Fig. 7(a). Thermocouple #9 was nearest to the fuel port surface. It may be observed that temperature difference

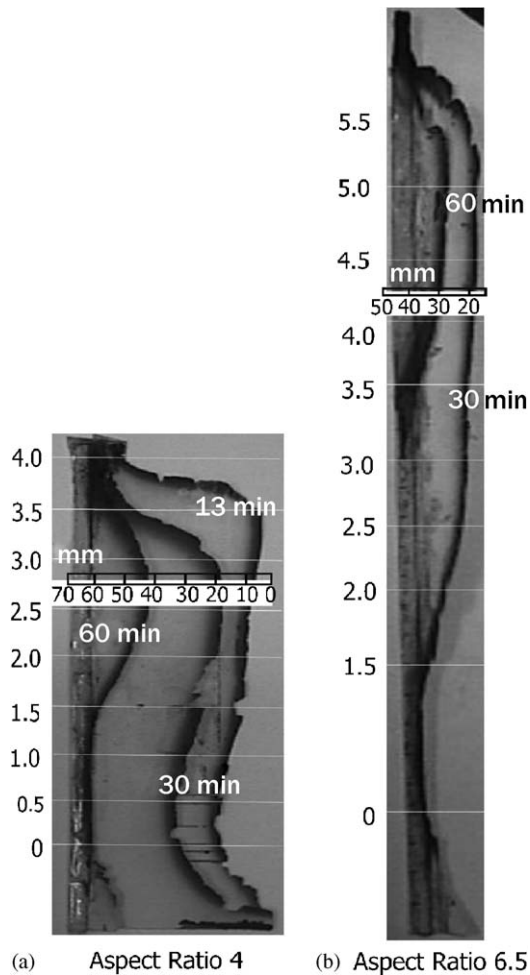


Fig. 5. Pyrolysis fronts extracted at various times from stoves of AR 4 and AR = 6.5.

between two locations has remained nearly constant after initial transients. Using the temporal distribution at various locations 1–9 of Fig. 7(a), the radial temperature profiles in c-phase at various times are plotted in Fig. 7(c). The axial coordinate chosen for the plot is a logarithmic scale. The reason for this choice is related to the expectation of the steady temperature distribution in adial coordinate geometry. Steady one-dimensional radial heat flow without heat generation in a solid cylinder is governed by heat conduction equation,  $(rT_r)_{,r}/r = 0$  where  $_{,r} = d/dr$ . For a hollow cylindrical geometry, with inner surface at  $r = a$  and outer surface at  $r = b$  and surface temperatures maintained  $T_s$  and  $T_o$ , respectively, the temperature distribution is given by  $\tau(r) = (T_s - T)/(T_s - T_o) = \ln(r/a)/\ln(b/a)$ , where  $\tau$  is the dimensionless temperature at any radius  $r$ . Therefore, logarithmic scale was chosen to plot distances in Fig. 7(c).

Experiments at various ARs and inlet configurations have revealed that flash back is an inevitable part of tube stove operation in the gasification mode. Table 1 consolidates information on the experiments made earlier and shows that in single port stoves flash back occurs beyond 30 min of stove operation.

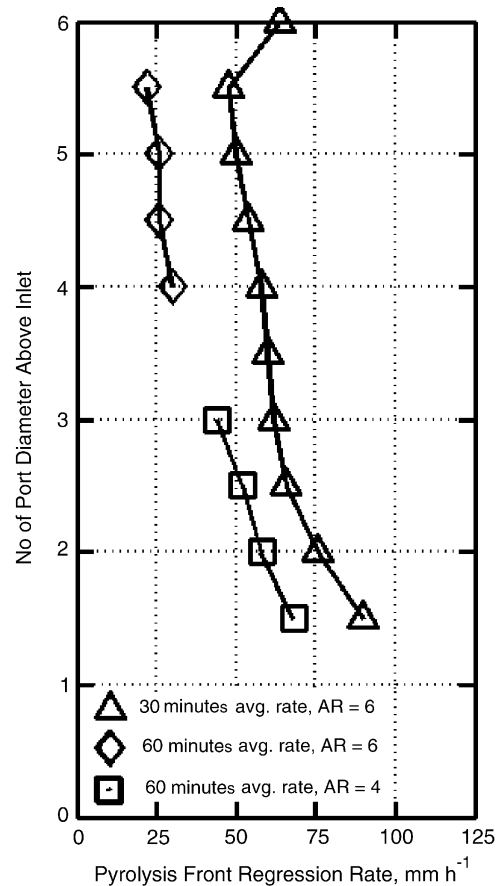


Fig. 6. Pyrolysis front movement rates as a function of vertical distance. Burnt paper sheet profiles from which this data is extracted is shown in Fig. 5(a) and (b).

Studies on efficiency consisted of the determination of the effect of spacing between bottom of the vessel and the exit of the stove on the overall heat utilisation efficiency of the stove. Efficiency was determined using standard procedures described in CIS 1315Z (part I) 1991 of Beureau of Indian Standards (BIS). The stove functioned at a nominal power level of 2.3 kW for which the prescribed vessel diameter is 200 mm and water quantity for each heating was 2 kg. The procedure consisted of repeatedly heating 2 kg of water at ambient temperature to a temperature 5 °C below boiling point using two sets of vessels alternatively. The vessels were stirred once just before attainment of required temperature. A total of 3–7 runs were required to completely extract useful energy present in the fuel block. Vessel was mounted on a threaded support as shown in the schematic diagram inset to Fig. 8 which also shows the water temperature and the weight loss record. It is seen that 2 kg of room temperature water could be heated to near boiling conditions in an average time of 13 min during the first hour of operation resulting in an efficiency of 37%. It was observed that increased gap brought down sooting tendency but heat utilisation efficiency was reduced. A gap of 12 mm was found to be optimal for operation.

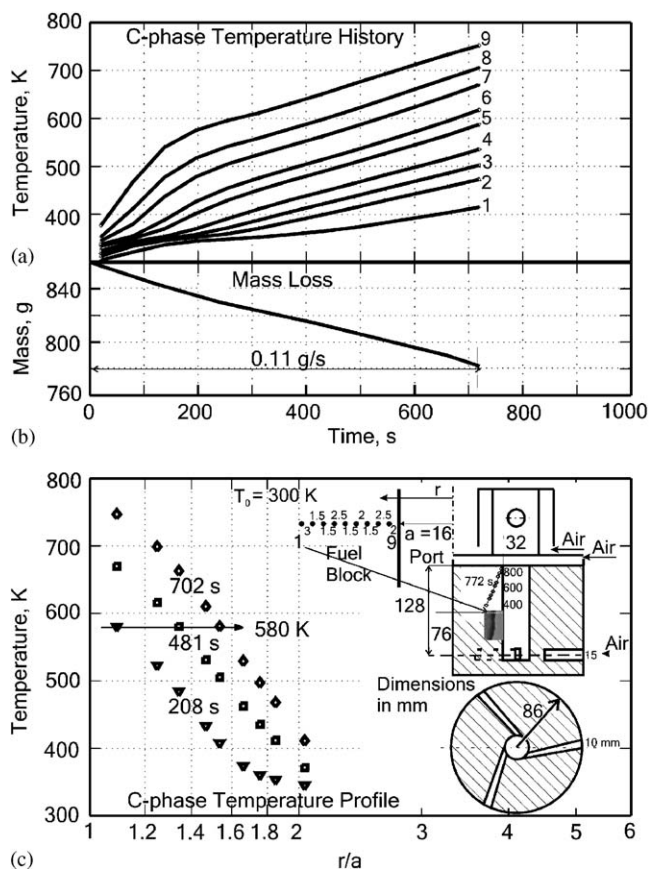


Fig. 7. C-phase temperature measurement (port diameter = 32 mm, AR = 4): (a) shows condensed phase temperature history. K type 100 μm diameter thermo-couples are used. Mass loss as a function of time is shown in (b). (c) shows condensed phase temperature profile at the location shown in schematic diagram.

Table 1  
Consolidated summary of experiments made on determination of causes of flash back

Port dia. (mm)	AR	Inlet area (mm <sup>2</sup> )	Flash back (min)
32	4.0	270	30
32	4.0	270	30
32	4.0	270	35
40	4.0	180	30
40	4.0	180	40
40	6.0	180	30
40	6.0	180	30
40	6.0	180	30
40	6.0	180	30
40	6.5	180	60
40	8.0	180	30
40	8.0	180	35
40	4.0	1250 (axial)	05
40	7.0	1250 (axial)	20

CO measurements were made using gas analyser with probe positioned at a distance of 30–45 cm from the burning stove and at a height of 30–37.5 cm from the ground level of the stove. The CO levels were less than the

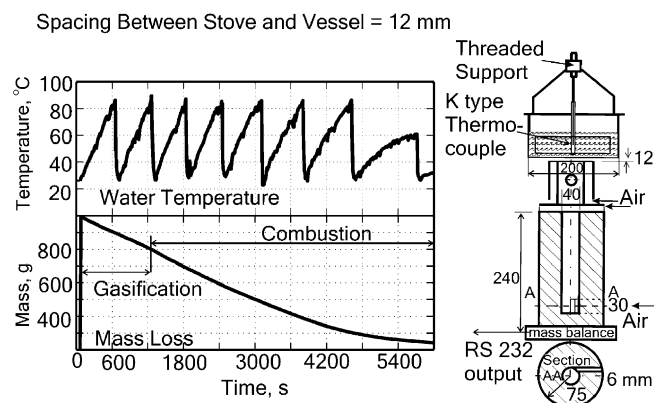


Fig. 8. Effect of spacing between stove and vessel on water boiling efficiency. Figure shows water temperature increase and corresponding mass loss of fuel for 12 mm spacing between stove and vessel.

9 and 35 ppm, limitation of national air quality standards (both primary and secondary) of USA as quoted by Mukunda et al. [10].

SPM in air surrounding stove was measured using an air quality meter which consisted of a vacuum pump with a flow meter connected to it. SPM content is found to be less than 2 mg m<sup>-3</sup>. This value is comparable to earlier measurements at 2.4 mg m<sup>-3</sup> reported by Mukunda et al. [10]. The actual kitchen SPM emission levels presented in [11] from their measurements in a number of kitchens are about 56 mg m<sup>-3</sup> maximum and 7 mg m<sup>-3</sup> average. The emission levels recorded in the present study is very low compared to these values.

Sooting tendency of the stove was also determined. This experiment was done in parallel with efficiency measurements. The soot collected at the bottom of the vessels used for water heating was cleaned using known mass of surgical cotton soaked in acetone. The soot collected is thus transferred to cotton. Cotton is dried in an oven and final mass is noted down to determine the mass of soot collected. Soot collected was about 2 g kg<sup>-1</sup> fuel. Only study available on sooting tendency was conducted by Mukunda et al. [10] who have reported upper limit of soot ~13 g kg<sup>-1</sup> fuel quantity for sun dry biomass with 12–15% moisture content.

#### 4. Multi-port studies

Studies on multi-port pulverised fuel stoves were taken up to overcome two major short comings of single port stoves. They were (a) re-ignition problems and (b) low fuel-to-energy conversion percentage in the required burn duration. For these studies, axial inlet port design was selected. This choice was based on the consideration that in the side inlet configuration, minor collapse of loose biomass from the upper region, if left unattended, led to increased restriction or even blockage of side air inlet resulting in the non-optimum stove performance. Whereas in axial inlet configuration of the type shown in Fig. 1(c)

the loose biomass always fell through with no possibility of blockage.

The typical structure of a fuel block having multiple fuel ports with axial inlets is shown in Fig. 1(c). In this configuration there is a central main port of larger diameter with 4 auxiliary satellite ports of smaller diameter. A flat plate with an arrangement for varying the distance from the bottom of the fuel block was provided as a control area to vary the possible air-to-fuel ratio for achieving gasification. This was helpful for placing a burning wick to facilitate ignition. Top of the fuel block was covered with a thin layer of ash which prevented indiscriminate lateral communication of ignition from the main port to side ports along the fuel block surface. A plenum volume vertically above the fuel block gave free passage to hot gases coming out of auxiliary ports into the device. The conical perforated plate placed above the device was used to carry out emission studies with a flat bottomed vessel placed over it. Three adjustable threaded supports shown in figure were used to optimise the spacing between the vessel and the plate.

Only the central port was ignited at the beginning of stove operation. A few drops of kerosene were sprinkled around the circumference of central port and also on to the small pile of fine fuel on the plate below the axial air inlet. Ignition was performed at the top first to create the draught and then on the pile of fine fuel at the bottom. Then the top cover is placed above the stove. By the time the pilot fuel was burnt up this process taking 3–5 min, the bottom region of the port became red hot and started generating volatiles allowing the stove to operate in the gasification mode. Gasification mode operation continued for about 20 min beyond which flame was observed within the main port. Operation of stove during this period was similar to single port stove.

Based on the pyrolysis front propagation data from single port studies, the auxiliary ports were so located that the pyrolysis front would reach these ports by 20 min of operation. Auxiliary ports were at a greater AR and delivered fuel rich gases which burnt at the exit in a stable diffusion mode. The partly burnt fuel streams from the auxiliary ports got drawn into the device due to the draft created by exiting region. A space between fuel block and the top device facilitated the free passage of gases from auxiliary ports to the device inlet. The excess fuel in the device region received part of the air necessary for oxidation through the central port as well as from the device. A small portion of the fuel also burnt beyond the stove exit. The port structure remained intact for almost entire flaming combustion duration. Towards the end of flaming combustion the structure around the central port was seen to disintegrate. By this time most of the biomass present in the stove was charred. This is indicative of the higher conversion percentages achieved in multi-port stoves.

The products of combustion from multi-port stove were tested for emissions of carbon monoxide and oxides of

nitrogen. For emission studies, four auxiliary port configuration of the kind shown in Fig. 1(c) was employed. Standard hood method was used for emission measurements. Moisture free sample gases were analysed for CO, NO<sub>x</sub> and O<sub>2</sub>. From this data, the emission factors of pollutants in kg (kg fuel)<sup>-1</sup> of known composition, were calculated using the method described in [12]. It was found that emissions were higher when the spacing between the vessel and the stove was low. This was probably due to flame quenching due to larger portion of reacting gases coming in contact with colder metal. Similar observations were also reported in [13,14]. Lower spacing is preferable from the point of view of achieving higher efficiency. Therefore, a study was conducted to optimise the spacing at which acceptable emission levels are achieved by varying the spacing between stove and vessel. This indicated that at a spacing of 12 mm between the vessel bottom and perforated guide plate at the bottom will have acceptable emission levels.

CO emission factors (see Fig. 9) of less than 17 g kg<sup>-1</sup> fuel have been recorded in the present study. The results of present study have demonstrated that lower emission at higher efficiencies is possible by adopting better combustion strategy in the form of phased air addition to the combustion zone. The hot product gases leave the stove through a narrow opening which results in focused delivery of energy that not only ensures complete combustion as the exit region is generally kept hot but also improves downstream heat transfer efficiencies.

NO<sub>x</sub> emission factors recorded from tube stoves are about 1 g kg<sup>-1</sup> fuel. This value is higher than those obtained in [12] but falls in the mid-range of the scattered values reported by [13] as seen in Fig. 10.

Over 25 experiments were conducted on multi-port stoves with varying configurations and it was found that the combustion was continuous without any flame-out in the multi-port operation. Fuel-to-energy conversion was in

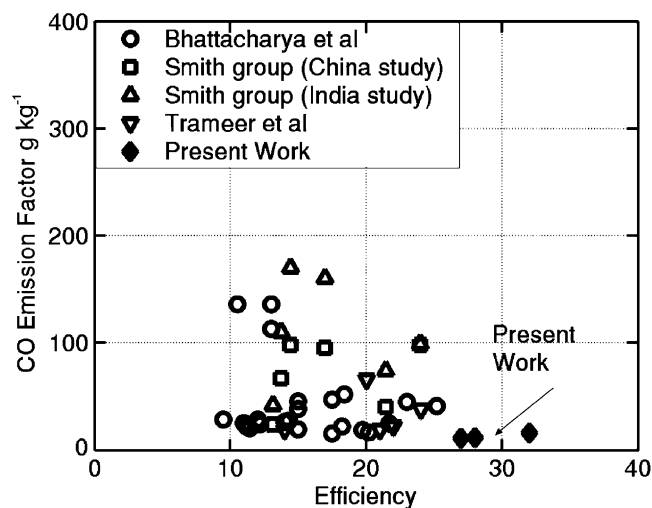


Fig. 9. Comparison of results from present work with CO emissions reported in Refs. [7,13,14,16].

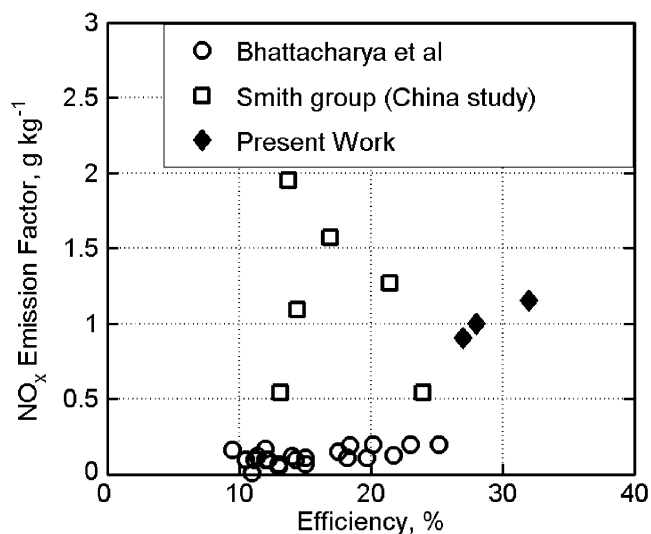


Fig. 10. Comparison of present work with NO emissions reported in Refs. [7,13].

the range of 66–73%. Higher conversion efficiencies were observed in fuel blocks with larger number of auxiliary ports. The increase in conversion efficiency between 4 and 6 ports was not appreciable. It appears multi-port tube stoves which are relatively simpler to construct and operate are viable options to obtain “clean” combustion coupled with high efficiencies using pulverised fuels.

## 5. Studies on pulverised fuels

This section is concerned with the studies on extending the utility of a tube stove to other fine fuels generated by pulverising leafy biomass. The objective is to evolve a strategy for the selection of suitable port geometry for bio-fuels with different characteristics.

Studies have been conducted in single port and multi-port configurations to determine the power levels achieved in similar configurations as well as the port configurations that were suitable for proper functioning with various fuels. Table 2 presents the proximate analysis of selected fuels and Table 3 presents ultimate analysis of selected fuels.

The performance of tube stove has been studied with varieties of pulverised leafy droppings in single port configuration. Of these, a comparative study of power levels from sawdust and pulverised acacia leafy droppings made at AR of 4 is reported. Under normal loading conditions the packing density of acacia was over  $400 \text{ kg m}^{-3}$ . This was due to high intrinsic density of fuel material ( $1000 \text{ kg m}^{-3}$ ) compared to sawdust.

A comparison of stove performance with similar configuration using acacia and sawdust as fuels is presented in Table 4.

The power level of operation was found to be 70% of sawdust stove ( $1.1 \text{ kW}_{\text{th}}$  instead of  $1.6 \text{ kW}_{\text{th}}$ ) at comparable degree of compaction. This was puzzling since the only

Table 2  
Proximate analysis of selected fuels (mass basis)

	Leucaena	Acacia	Sawdust
Moisture (%)	10.0	10.0	10.0
Volatile matter (%)	64.0	58.9	65.7
Fixed carbon (%)	21.3	22.5	21.5
Ash (%)	4.7	8.6	2.8

Table 3  
Ultimate analysis of selected fuels (mass basis)

Species	C (%)	H (%)	N (%)	O (%)	Ash (%)
Leucaena	47.90	6.00	0.70	40.22	5.18
Acacia	44.20	4.90	0.90	40.48	9.52
Sawdust	47.30	6.10	0.70	42.79	3.11

recognisable difference from sawdust stove at that juncture was the difference in loading density of the fuel and expected behaviour was denser pulverised fuel should still generate comparable power output as mass flux from pyrolysis front, given by  $\rho_p \dot{r}$  was expected to remain same, with increase in  $\rho_p$  getting compensated by decreased  $\dot{r}$  (this is because all thermal balance equations have  $\rho_p \dot{r}$  as the term; therefore, the surface heat balance allows one to get  $\rho_p \dot{r}$ , for instance, see [15]).

A similar comparative study between performances of tube stove with pulverised leucaena pod and sawdust in a multi-port configuration was also conducted. The geometry employed for this study was similar to the one shown in Fig. 1(c). Experimental details are presented in Table 5.

It is seen that the power levels obtained with leucaena as fuel is about 75% of the power level obtained in a similar geometry with sawdust as fuel as seen in Table 5.

In case of pulverised leafy fuels, the port size on extraction of the tube around which the fuel block formed became slightly smaller than the diameter of the tube used to construct the port. This tendency was also present in sawdust but to a lower extent. This resulted in reduced size fuel ports for pulverised leafy biomass fuels. Initially, it was thought the reduction in power level was due to this reduction in port size. Therefore to offset this, the tube used to form fuel port was chosen to be slightly larger than the required port size. This did not appreciably increase the power level of operation.

Therefore, it was decided to conduct a thermo gravimetric analysis of different pulverised fuels used in the stove to determine the thermo chemical behaviour of these fuels. A constant heating rate of  $10^\circ \text{C min}^{-1}$  was employed for all fuels. Ash content of the fuel was also separately determined. Results are presented in Fig. 11.

It is seen that volatilisation rate of pulverised leucaena pod is 75% of sawdust (see Fig. 11). Packing densities of both fuels are similar. The relative power level obtained from leucaena fuel block compared to sawdust fuel block

Table 4  
Comparison of acacia and sawdust

Sl no.	$d$ (mm)	AR	$\rho$ ( $\text{kg m}^{-3}$ )	$m_i$ (kg)	0–30 min		0–60 min		$t_g$ (min)	Data
					% (mass)	Power (kW)	% (mass)	Power (kW)		
19	32	4.0	425	1.50	10.4	1.0	17.7	1.1	—	Acacia
25	32	4.0	240	0.82	21.7	1.6	44.7	1.6	—	Sawdust

Table 5  
Comparison of 4 auxiliary port stoves with leucaena and sawdust as fuels

Sl no.	Main dia.	Aux. port		AR <sup>a</sup>	$\rho$ ( $\text{kg m}^{-3}$ )	$m_i$ (kg)	Power (kW)	Conv. (%)	$t_b$ (min)	Fuel
		Dia.	No.							
1	35	18	4	6	230	0.7	3.2	72	40	Sawdust
2	35	18	4	6	230	0.7	2.4	72	55	Leucaena

<sup>a</sup>Based on main port diameter.

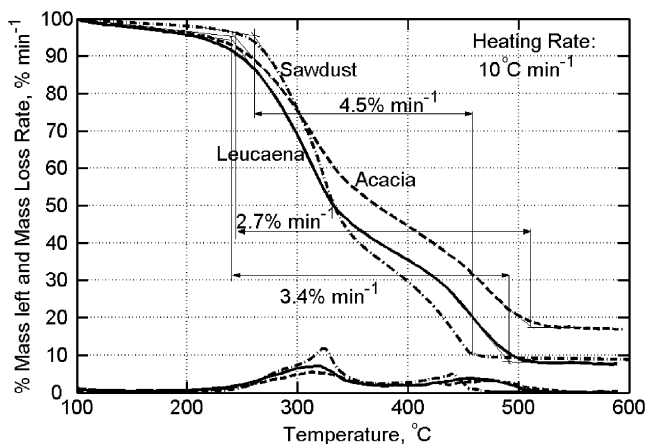


Fig. 11. Thermo gravimetric analysis of selected pulverised leafy fuels.

of similar geometry was 79% during gasification mode operation and 73% during combustion mode operation. From this it was inferred that low average volatilisation rates were responsible for the lower power level operation of leucaena compared to sawdust.

Volatilisation rate of acacia is 60% of sawdust as seen from Fig. 11. The power obtained from acacia fuel block was 70% of a similar sawdust fuel block during gasification mode operation and 71% during combustion mode operation. The relative power from acacia fuel block is higher than the relative volatilisation rate. Packing density of acacia fuel is  $430 \text{ kg m}^{-3}$ . Particle density of acacia leafy fuel is  $1000 \text{ kg m}^{-3}$ . This resulted in a fuel bed with higher porosity compared to sawdust with intrinsic density  $560 \text{ kg m}^{-3}$  packed to  $230 \text{ kg m}^{-3}$ . The effect of lower degree of compaction is to increase power level of operation as discussed in Section 3. Due to larger porosity, stove with acacia fuel has exhibited a relative power level higher than the relative volatilisation rate compared to sawdust.

A comparative study of performance of stove with pulverised acacia as fuel using 4 and 6 aux. ports has also been made. For this study lower AR was selected. This was done for two reasons. The combustion of pulverised acacia, with AR based on main port greater than 4, was in a fuel—rich regime. Therefore an AR of 2.5 (based on main port) was selected for this study. It was found that at this AR, stable clean combustion could be established as most of the fuel port was active and the head causing air flow was also lower. Experimental details are presented in Table 6.

It is seen that power level of operation of 6 auxiliary port configuration was higher than 4 auxiliary port. Also the conversion fraction of 4 aux. port (48%) was low compared to 6 aux. port (58%) configuration. This must be compared with the increase in conversion percentages obtained between 4 and 6 port configurations with sawdust as fuel which was just by 1%. This implies provision of larger fuel surface areas would lead to higher conversion fractions in case of fuels with lower average volatilisation rates.

## 6. Summary

It is found that gasifier stove functions in gasification mode for about 30 min. A variety of pulverised fuels can be used in tube stoves in single port and multi-port configurations. Pulverised fuels of leafy origin have low volatilisation rates and hence exhibit lower power level operations in comparable geometries. Also, in multi port configurations at higher AR with axial inlets, the combustion at exit tended to be smoky due to partial flame outs caused by larger amounts of air traversing the core. Therefore, lower AR geometries were successfully employed to achieve clean combustion. Required power levels of operation could be achieved by increasing the port diameters. The stove has performed excellently at water

Table 6  
Comparison of 4 auxiliary port and 6 auxiliary port stoves with acacia as fuel

Sl no.	Main dia.	Aux. port		AR <sup>a</sup>	$\rho$	$m_i$ (kg)	Power (kW)	Conv. (%)	$t_b^b$ (min)	Fuel
		Dia.	No.							
1	35	18	4	2.5	230	0.62	1.5	48	50	Acacia
2	35	18	6	2.5	230	0.62	1.8	58	50	Acacia

<sup>a</sup>Based on main port diameter, all dimensions in mm.

<sup>b</sup>Burn time.

boiling efficiencies as high as 37% at near constant power level. Emission performance is also very good with CO emission as low as 17 g kg<sup>-1</sup> fuel.

## References

- [1] Mukunda HS, Dasappa S, Swati B, Shrinivasa U. Studies on stove for powdery biomass. *International Journal of Energy Research* 1993;17:281–91.
- [2] Mukunda HS, Dasappa S, Paul PJ, Rajan NKS, Shrinivasa U. Gasifiers and combustors for biomass—technology and field studies. *Energy for Sustainable Development* 1994;1(3):27–38.
- [3] Ohlemiller TJ. Modeling of smouldering combustion propagation. *Progress in Energy and Combustion Science* 1985;11(4):277–310.
- [4] Ohlemiller TJ. Smouldering combustion. In: Society of fire protection engineers' hand book of fire protection engineering. National Fire Protection Association; 1995.
- [5] Williams FA. Mechanism of fire spread. Sixteenth Symposium (International) on Combustion 1976;11(1281–1294):277–310.
- [6] Blasi CD. Modeling and simulation of combustion processes in charring and non-charring solid fuels. *Progress Energy Combustion Science* 1993;19(1281–1294):71–104.
- [7] Bhattacharya SC, Albina DO, Salam AP. Emission factors of wood and charcoal fired cookstoves. *Biomass and Bioenergy* 2002;23:453–69.
- [8] Anon. Indian improved cookstoves: a compendium. Field Document 41, Regional Wood Energy Development Programme in Asia, Bangkok Thailand, July 1993.
- [9] Dixit CSB. Experimental and computational studies on a pulverized fuel stove. PhD thesis, Bangalore, India: Indian Institute of Science, 2003.
- [10] Mukunda HS, Shrinivasa U, Dasappa S. Portable single-pan wood stoves for high efficiency. *Sadhana* 1988;13(4):237–70.
- [11] Smith KR, Aggarwal AL, Dave RM. Air pollution and rural biomass fuels in developing countries: a pilot study in India and implications for research and policy. *Atmospheric Environment* 1983;17:2343–62.
- [12] Bhattacharya SC, Albina DO, Khaing AM. Effects of selected parameters on performance and emission of biomass-fired cookstoves. *Biomass and Bioenergy* 2002;23:387–95.
- [13] Zhang J, Smith KR, Ma Y, Ye S, Jiang F, Qi W, et al. Greenhouse gases and other airborne pollutants from household stoves in china: a database for emission factors. *Atmospheric Environment* 2000;34:4537–49.
- [14] Ballard-Trameer G, Jawurek HH. Comparison of five rural wood-burning cooking devices: efficiencies and emissions. *Biomass and Bioenergy* 1996;11(5):419–30.
- [15] Mukunda HS. Understanding combustion. IIT Madras series in science and engineering. Amsterdam: Macmillan India Limited; 1989.
- [16] Smith KR, Uma R, Kishore VVN, Lata K, Joshi V, Zhang J, et al. Greenhouse gases from small-scale combustion devices in developing countries. Phase 2a: Household stoves in India. Report for USEPA, November 1998.